



HAL
open science

Experimental investigation of the crash energy absorption of 2.5D-braided thermoplastic composite tubes

Cyril Priem, Ramzi Othman, Patrick Rozycki, Damien Guillon

► **To cite this version:**

Cyril Priem, Ramzi Othman, Patrick Rozycki, Damien Guillon. Experimental investigation of the crash energy absorption of 2.5D-braided thermoplastic composite tubes. *Composite Structures*, 2014, 116, pp.814-826. 10.1016/j.compstruct.2014.05.037 . hal-01240159

HAL Id: hal-01240159

<https://hal.science/hal-01240159>

Submitted on 12 Mar 2017

HAL is a multi-disciplinary open access archive for the deposit and dissemination of scientific research documents, whether they are published or not. The documents may come from teaching and research institutions in France or abroad, or from public or private research centers.

L'archive ouverte pluridisciplinaire **HAL**, est destinée au dépôt et à la diffusion de documents scientifiques de niveau recherche, publiés ou non, émanant des établissements d'enseignement et de recherche français ou étrangers, des laboratoires publics ou privés.

Public Domain

Experimental investigation of the crash energy absorption of 2.5D-braided thermoplastic composite tubes

Cyril Priem^a, Ramzi Othman^{a,b}, Patrick Rozycki^a, Damien Guillon^c

^aLUNAM Université, Ecole Centrale de Nantes, Institut de Recherche en Génie Civil et Mécanique (GeM), UMR CNRS 6183, BP 92101, 44321 Nantes cedex 3, France

^bMechanical Engineering Department, Faculty of Engineering, King Abdulaziz University, P.O. Box 80248, Jeddah 21589, Saudi Arabia

^cCETIM/pôle Ingénierie Polymères & Composite, Technocampus EMC2, Z.I. du Chaffault, 44340 Bouguenais, France

Braided composites tubes have been reported to have a great potential in crash energy absorption applications. However, previous works were limited to thermoset braided composite tubes. In this study, we are interested in the crash energy absorption performance of 2.5D braided thermoplastic composite tubes. The sensitivity to materials, fiber orientation and geometry was investigated. Three crushing modes have been observed. The splaying and progressive folding were reported for glass/polypropylene tubes and fragmentation mode was observed for carbon/polyamide tubes. The last mode has the highest specific energy absorption of 61 kJ/kg. The progressive folding mode has higher specific energy absorption (36 kJ/kg) than the splaying mode. Moreover, the specific energy absorption increases with increasing braiding angle and decreasing length-to-diameter ratio, for glass/polypropylene tubes. On the opposite, the specific energy absorption decreases with braiding angle for carbon/polyamide tubes.

Keywords:

Crashworthiness
Specific energy absorption
Crushing modes
Braided composites
Thermoplastics

1. Introduction

Replacement of metals by composite materials in structural parts becomes a real challenge for industrialists because of the crucial need to create lighter vehicles. A major difficulty is to understand the dynamic behavior of composite structures such as energy absorbers. They must absorb a high amount of energy during a crash and have a stable way to do it. Originally they are made of metallic materials. But the high properties of composite materials make them very attractive to improve performance and decrease fuel consumption [1].

The mechanical behavior of tubes made of metals has been well studied and understood [2–12]. The energy is dissipated by plastic deformation, creating symmetrical or non-symmetrical progressive buckling. Metallic materials are easily simulated which allow a complete and costless knowledge of the behavior of a structure and of the influence of the different parameters, such as trigger [6]. Different attempts have been made to combine metallic and composite materials to create composite tubular structures, such

as filling metallic tubes with foams [11] or by wrapping them with fibers [12].

Energy absorbers completely made of composite materials have been proposed [13,14]. Because of their lower viscosity, thermoset reinforced composite tubes were widely used and studied [15–27]. Different modes of crushing have been identified, such as splaying and fragmentation modes [20]. The crushing modes and consequently the specific energy absorption are dependent on multiple parameters such as the tube geometry [28–32], fiber type [33,34] and architecture [31,32], matrix resin [35], testing speed [32,36,37], temperature [38], trigger [39,40] and surface treatment [41]. Recently, Mahdi and Sebaey [42] have reported that radial reinforcements improve crashworthiness capabilities. Besides, some studies have investigated the absorption capabilities of natural fibers reinforced polymer composite tubes [43–46].

The use of reinforced thermoplastic composite materials for energy dissipation has received less attention [40,41,47–53]. Hamada et al. [47] achieved a specific energy absorption as high as 180 kJ/kg with unidirectional carbon fiber/PEEK composite tubes. Therefore, high crashworthiness performances can be expected from composite materials. Hamada et al. [50] split the absorbed energy into the energy dissipated in longitudinal cracking of walls, the energy required for splitting of fronds into beams, the energy needed for fiber fracture, the energy dissipated in frictional heating and some others. They also attributed the high

value carbon/PEEK tubes' specific energy absorption to the higher fracture toughness of the carbon/PEEK composite material. Hamada et al. [49] showed that rapid cooling of carbon/PEEK leads to 15% higher specific energy absorption than gradual and slow cooling. Hamada and Ramakrishna [51] investigated fiber material effects and founded that specific energy absorption of carbon/PEEK composite boxes is 20% higher than glass/PEEK tubes. In terms of fiber orientation effects, the highest specific energy (225 kJ/kg) is achieved with tubes having ± 15 fiber orientation [52]. Ramakrishna et al. [50] concluded that carbon/PEEK tubes have the highest energy absorption capability compared to carbon/PEI (188 kJ/kg), carbon/PI (168 kJ/kg) and carbon/PAS tubes (148 kJ/kg). Zarei et al. [53] were interested in woven glass fiber polyamide composite square and hexagonal tubes. The highest specific energy absorption (~ 56 kJ/kg) is obtained for the thicker square tubes. However, higher crash load efficiency is obtained for hexagonal tubes.

A limitation of the use of composites in crash is the phenomenon of delamination. In laminated composites, the bond between

the layers is only assured by the matrix which allows failure without dissipating a significant amount of energy. Composite materials with 2.5D fibers architecture avoid this problem by creating through-the-thickness reinforcements. Refs. [44–66] have already investigated the energy absorption capability of braided thermoset composite tubes, including triaxial preform design as “3D-braid”. The use of 2.5D structured composite materials with through the thickness reinforcement can enhance energy absorption performances of braided structures.

The purpose of this article is to study crash energy absorption capability of circular 2.5D-braided thermoplastic composite tubes. Two composite materials have been considered: glass fibers associated with polypropylene matrix and carbon fibers with polyamide matrix. The influence of braiding fibers orientation has also been studied. The different modes of crushing are described and the performances of energy absorption have been calculated. *To the best of author's knowledge, this is the first time that the crashworthiness efficiency, of 2.5D-braided composite tubes, and moreover with thermoplastic resin is investigated.*



Fig. 1. Overview of the experimental setup.

Table 1
Testing conditions for glass/polypropylene tubes.

Name	Length (mm)	Orientation (°)	Impact angle (°)	Impact speed (m/s)	Chamfer
V2-20-1	200	20	0	8.17	45°
V2-20-2	200	20	0	8.17	45°
V-20-1	110	20	0	4.9	45°
V-20-2	110	20	0	5	Flat
V-20-3	110	20	15	4	45°
V-20-4	110	20	15	4	Flat
V-20-5	110	20	15	4	45°
V-20-6	110	20	0	4.9	45°
V2-45-1	200	45	0	8.17	45°
V2-45-2	200	45	0	8.17	45°
V-45-1	110	45	0	5	45°
V-45-2	110	45	0	5	Flat
V-45-3	110	45	15	4	45°
V-45-4	110	45	15	4	Flat
V2-75-1	200	75	0	8.17	45°
V2-75-2	200	75	0	8.17	45°
V-75-1	110	75	0	5.2	45°
V-75-2	110	75	0	5	Flat
V-75-3	110	75	15	4	45°
V-75-4	110	75	15	4	Flat

Table 2
Testing conditions for carbon/polyamide tubes.

Trial	Length (mm)	Orientation (°)	Impact angle (°)	Impact speed (m/s)	Chamfer
C-30-1	110	30	0	5.2	45°
C-30-2	110	30	0	7.1	45°
C-30-3	110	30	15	4.5	45°
C-30-4	110	30	0	7	45°
C-45-1	110	45	0	7	45°
C-45-2	110	45	0	7.1	45°
C-45-3	110	45	0	7	45°
C-45-4	110	45	15	4	45°
C-45-5	110	45	0	7	45°
C-45-6	110	45	0	7	45°

2. Method

2.1. Experimental setup

Crushing tests were carried out by using a drop-weight tower (Fig. 1). A total weight of 319 kg was dropped from a height between 0 and 3.5 m to achieve impact velocities up to ~ 8 m/s. The composite tubes were riveted to an intermediate metallic plate, which is fixed on the bottom support, instrumented by a force transducer, through four screws. The experimental setup was also instrumented by a Photron SA1 high speed video camera. Images were stored at a frequency rate of 4000 pictures per second. The tracking software TEMA motion is used to determine the displacement of the falling mass which is called the striker henceforth. Both the force transducer and the video camera were synchronized by using a home-made trigger. Force measurements were initially recorded using a sampling rate of 1 MHz. Subsequently, the step time of force signals was aligned with the step time of displacement signals, i.e., 250 μ s.

2.2. Composite tubes and impact loading

Two materials have been used. The first one is named Twintex and produced now by Fiber Glass Industries. It is made of a comingled glass fibers and polypropylene matrix. The second one is a comingled carbon fibers and polyamide matrix produced by COM-FIL. The 2.5D-braided reinforcements were realized by DJP with ply by ply interlocked bias fibers. In terms of the glass fiber reinforced composite, three different fiber configurations were produced:

- 240 doubled axial fibers and 80 simple fibers oriented at $\pm 75^\circ$,
- 320 doubled axial fibers and 320 simple fibers oriented at $\pm 45^\circ$, and
- 320 doubled axial fibers and 320 simple fibers oriented at $\pm 20^\circ$.

For the carbon fiber/polyamide composite, two reinforcement architectures were considered. Namely,

- 320 doubled axial fibers and 320 simple fibers oriented at $\pm 45^\circ$, and
- 320 doubled axial fibers and 320 simple fibers oriented at $\pm 30^\circ$.

All tubes were braided on a 120 mm-mandrel and consolidated under an air-empty bag in an oven. A temperature of 210 °C has been reached for glass fiber/polypropylene tubes and 260 °C for carbon fiber/polyamide boxes. A thermal duct was used to avoid folds of the braided composite.

The composite cylindrical tubes are either 100 or 200 mm long. The inner and outer diameters are 116.5 and 123.5 mm, respectively. Some tubes have 45° chamfers, the others have flat ends. Two impact angles were investigated: 0° (axial impact) and 15°. Information on fiber orientation, tube length, trigger, impact angle

and impact velocity, per test, are detailed in Tables 1 and 2 for braided glass/polypropylene and carbon/polyamide, respectively, composites tubes.

2.3. Analysis

The dropweight tower used for this experimental study was instrumented with a force transducer and a high speed video camera. For each experiment, the force signal $F(t)$ and a sequence of digital images were stored on a computer. These images were first analyzed qualitatively to understand the crushing mechanism. Subsequently, tracking software is used to determine the displacement $\delta(t)$ of the dropped mass or the striker. The crashworthiness efficiency of the braided composite tubes are investigated in terms of two parameters: the crash efficiency parameter η and the specific energy absorption SEA. Fig. 2 depicts a typical load-displacement curve. The crush Efficiency is defined as the average-to-maximum forces ratio. Namely,

$$CE = \frac{F_{avg}}{F_{max}} = \frac{\int_0^{\delta_{max}} F d\delta}{\delta_{max} F_{max}} \quad (1)$$

where δ_{max} is the maximum consumed length, F_{max} is the peak force and F_{avg} is the mean force. This ratio should be close to 1 in order to avoid overstressed conditions in the material while absorbing energy. The average force is proportional to the absorbed energy whereas the maximum force is proportional to maximum mass deceleration. Consequently, the crush efficiency parameter highlights the capability of absorbing energy while keeping acceptable deceleration.

The second parameter is the Specific Energy Absorption. It is defined as the absorbed energy-consumed mass ratio, i.e.,

$$SEA = \frac{W}{\rho A \delta_{max}} = \frac{\int_0^{\delta_{max}} F d\delta}{\rho A \delta_{max}} \quad (2)$$

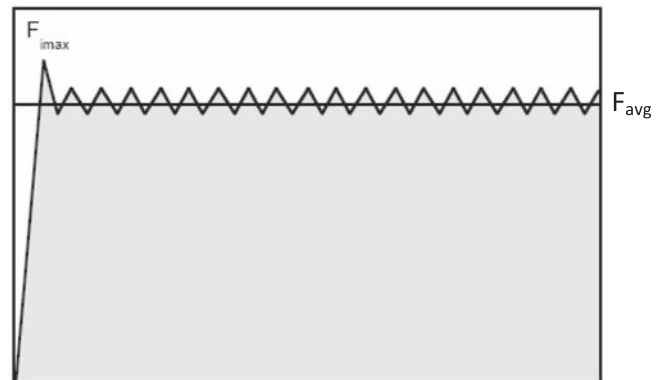


Fig. 2. Schematic of the load-displacement curve.

where W , ρ and A hold for the absorbed energy, composite material density and cross-sectional area of the tube, respectively. In other words the specific energy absorption is defined as the absorbed energy per consumed mass. The higher the specific energy absorption is, the lighter is the absorber.

The absorbed energy is determined by the area under the force-displacement curve:

$$\left(W = \int_0^{\delta_{\max}} F d\delta \right)$$

In this paper, only the post-peak part of the force-displacement curve is considered as this part represents the stable crushing process. Thus, the specific energy absorption is determined by

$$SEA = \frac{\int_{\delta_1}^{\delta_2} F d\delta}{\rho A (\delta_2 - \delta_1)} \quad (3)$$

where $[\delta_1, \delta_2] \subset [0, \delta_{\max}]$ is the interval of stable crushing. This way we can avoid the influence of the peak force that highly depend on the trigger.

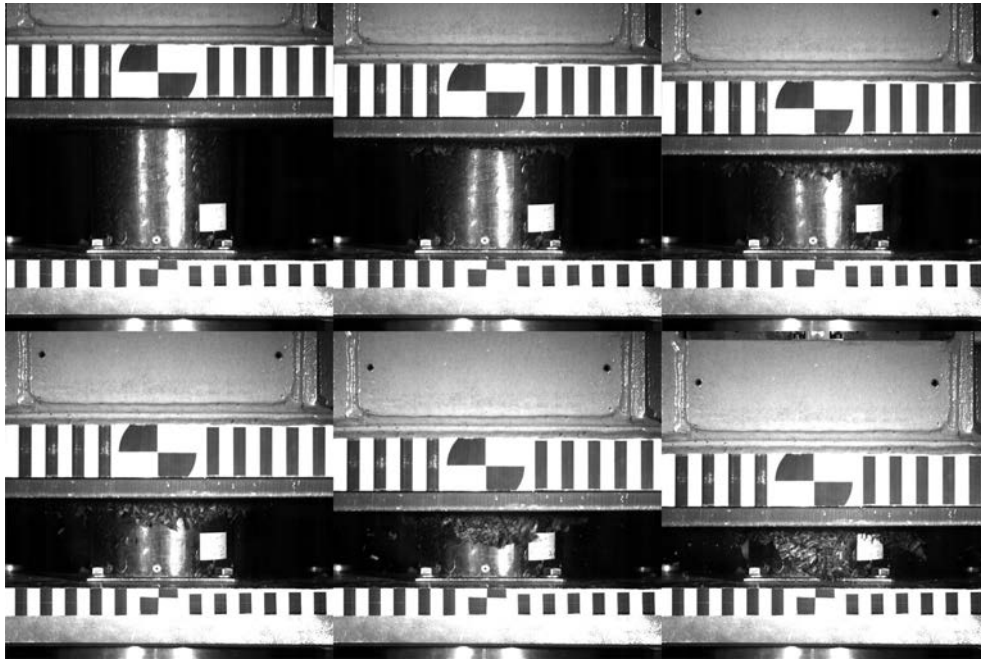


Fig. 3. Crushing process of a glass fibers composite tube at an impact angle of 0° (test: V-75-2).



Fig. 4. Examples of crushing modes of continuous fibers composite tubes at 0° of impact angle: folding mode on the high left (V2-75-1), splaying on the high right (V2-20-1), splaying in 4 parts on the bottom left (V2-45-2) and fragmentation on the bottom right (C-30-1).

3. Results

3.1. Crushing modes

Three stable modes of breaking have been identified: fragmentation, splaying and folding with extensive matrix failure between roving and rare delamination. Fig. 3 depicts the crushing sequence

Table 3
Crushing modes for glass/polypropylene tubes (impact angle 0°).

Name	Orientation (°)	Trigger	Crushing mode
V2-20-1	20	Yes	Splaying
V2-20-2	20	Yes	Splaying
V-20-1	20	Yes	Splaying + delamination
V-20-2	20	No	Unstable: Euler folding
V-20-6	20	Yes	Splaying + delamination
V2-45-1	45	Yes	Splaying
V2-45-2	45	Yes	Splaying in 4 parts
V-45-1	45	Yes	Progressive folding + splaying + delamination
V-45-2	45	No	Splaying at the bottom (breaking of the rivets)
V2-75-1	75	Yes	Progressive folding
V2-75-2	75	Yes	Progressive folding + splaying in 4 parts
V-75-1	75	Yes	Progressive folding
V-75-2	75	No	Progressive folding

obtained with test V-75-2 (Table 2). A progressive folding process was observed.

In terms of glass/polypropylene tubes, the axial crushing (impact angle equal to 0°) is mainly dominated by two stable modes, namely, splaying and progressive folding (Fig. 4 and Table 3). However, the absence of trigger can lead to an unstable failure mechanism. The crushing mode is governed by the orientation of the fibers. Indeed, the crushing deformation of tubes, with through-the-thickness bias fibers oriented at $\pm 20^\circ$ and $\pm 45^\circ$, is dominated by the splaying mode (Table 3). On the other hand, the progressive folding mode is mainly recorded for tubes with through-the-thickness bias fibers oriented at $\pm 75^\circ$. The crushing is however independent of tube's length or the length-to-diameter ratio (Table 3).

The off-axis crushing modes are given in Table 4 and some examples are shown in Fig. 5. Similarly to the axial crushing, the splaying mode is observed for $\pm 20^\circ$ and $\pm 45^\circ$ fiber orientation whereas the progressive folding mode is observed for $\pm 75^\circ$ fiber orientation. At $\pm 20^\circ$, fragmentation occurs at the beginning of test (except for test V-20-5). However, the splaying and progressive folding modes are superposed to tube bending at $\pm 45^\circ$ and $\pm 75^\circ$, respectively.

For carbon/polyamide tubes, the fragmentation crushing mode is dominating the failure mechanism at 0° impact angle (Fig. 4 and Table 5). This is independent of fiber orientation and trigger.

Table 4
Crushing modes for glass/polypropylene tubes (impact angle 15°).

Name	Orientation (°)	Trigger	Crushing mode
V-20-3	20	Yes	Fragmentation at the beginning then splaying
V-20-4	20	No	Fragmentation at the beginning then splaying
V-20-5	20	Yes	Bending without breaking + splaying
V-45-3	45	Yes	Bending without breaking + splaying
V-45-4	45	No	Bending without breaking + splaying
V-75-3	75	Yes	Bending without breaking + splaying + progressive folding between
V-75-4	75	No	Bending without breaking + splaying + progressive folding between

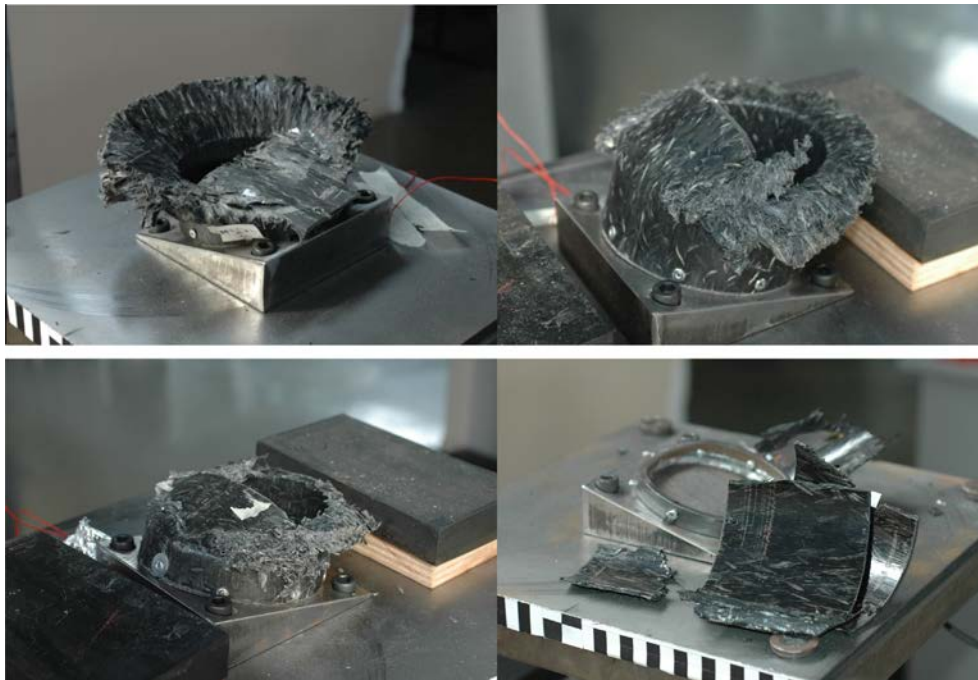


Fig. 5. Examples of crushing modes of continuous fibers composite tubes at 15° of impact angle: bending with rupture on the high left (V-20-3), without on the high right (V-45-3), bending and splaying on the bottom left (V-75-3) and catastrophic failure on the bottom right (C-30-3).

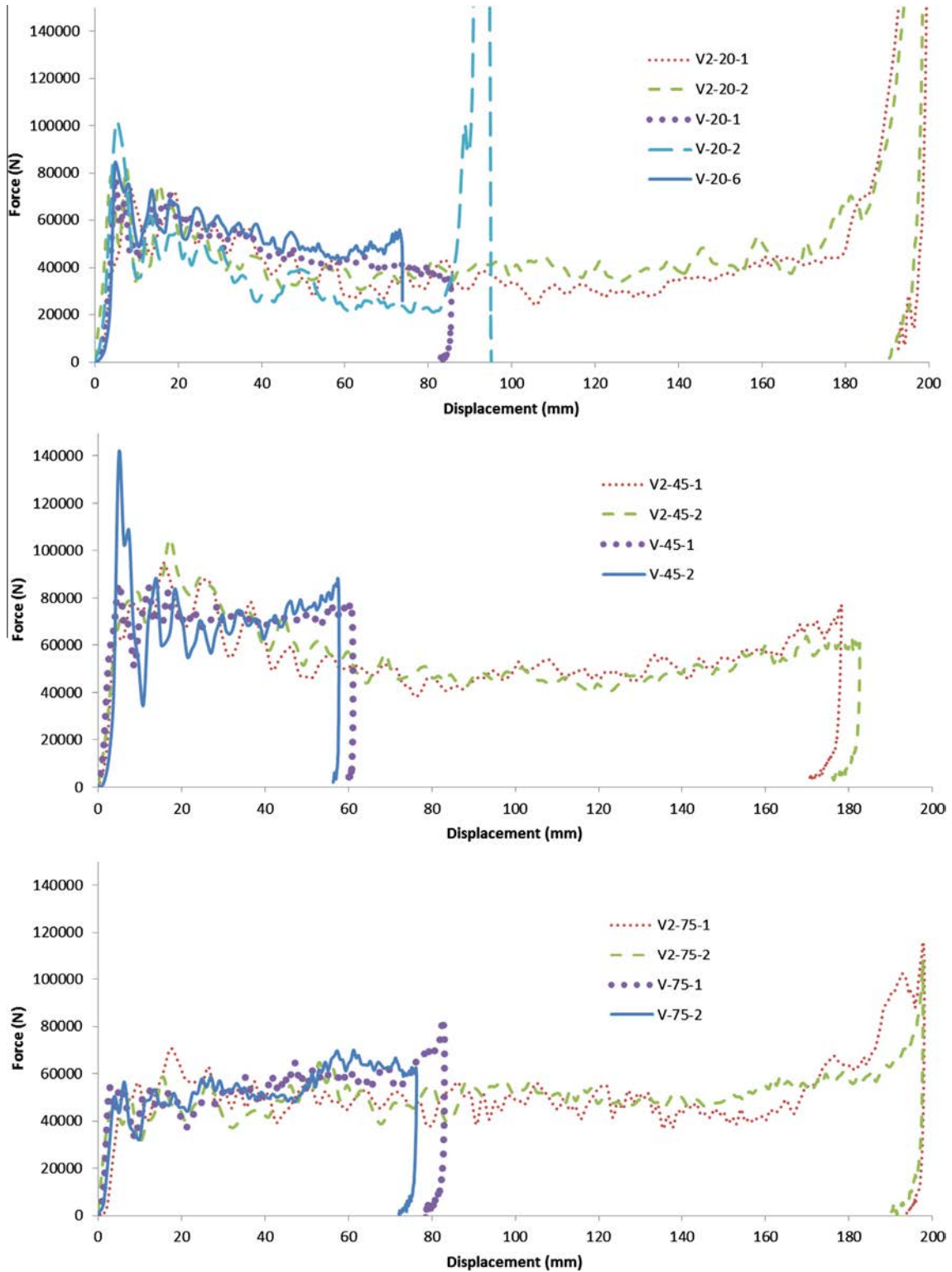


Fig. 6. Force–displacement curves for glass/polypropylene tubes (impact angle 0°) with through-the-thickness fibers orientated at $\pm 20^\circ$ (top), $\pm 45^\circ$ (middle) and $\pm 75^\circ$ (bottom).

Some splaying is also recorded for experiments. On the other hand, the off-axis crushing is dominated by a catastrophic failure (Fig. 5).

3.2. Force–displacement curves

Firstly, we are interested in the axial crushing of glass/polypropylene tubes. Force–displacement curves are shown in Fig. 6. Three

stages were observed. In the first stage, the force rapidly increases to a peak force. This is followed by a stable crushing part. By the end of some test, densification is recorded if the crushed distance approaches the total tube’s length. The peak force highly depends on the trigger. Unchamfered tubes have higher peak forces mainly for the splaying crushing mode, i.e., for $\pm 20^\circ$ and $\pm 45^\circ$ fiber oriented tubes. The peak force is also dependent on the crushing

Table 5
Crushing modes for carbon/polyamide tubes (impact angle 0°).

Name	Orientation (°)	Crushing mode
C-30-1	30	Fragmentation + some splaying
C-30-2	30	Fragmentation + some splaying
C-30-4	30	Fragmentation + some splaying
C-45-1	45	Fragmentation + some splaying
C-45-2	45	Fragmentation + some splaying
C-45-3	45	Fragmentation + some splaying
C-45-5	45	Fragmentation + some splaying
C-45-6	45	Fragmentation + some splaying

modes and/or fiber orientation. More precisely, the splaying mode ($\pm 20^\circ$ and $\pm 45^\circ$) leads to higher peak forces than the progressive folding mode ($\pm 75^\circ$). The post-peak stage (steady crushing part) is also depending on fiber orientation. For $\pm 20^\circ$ and $\pm 45^\circ$ orientations (except for 110 mm-long tubes with fibers at $\pm 45^\circ$), the force is oscillating around a mean force that is softly decreasing. For $\pm 75^\circ$ orientation, the force is rather oscillating a constant mean force.

Fig. 7 depicts the axial crushing force–displacement curves of carbon/polyamide composite tubes. During the first stage, the force rapidly increases in terms of displacement up to a peak force. Subsequently, the force oscillates around a constant mean force during the steady crushing stage. The peak force is much higher

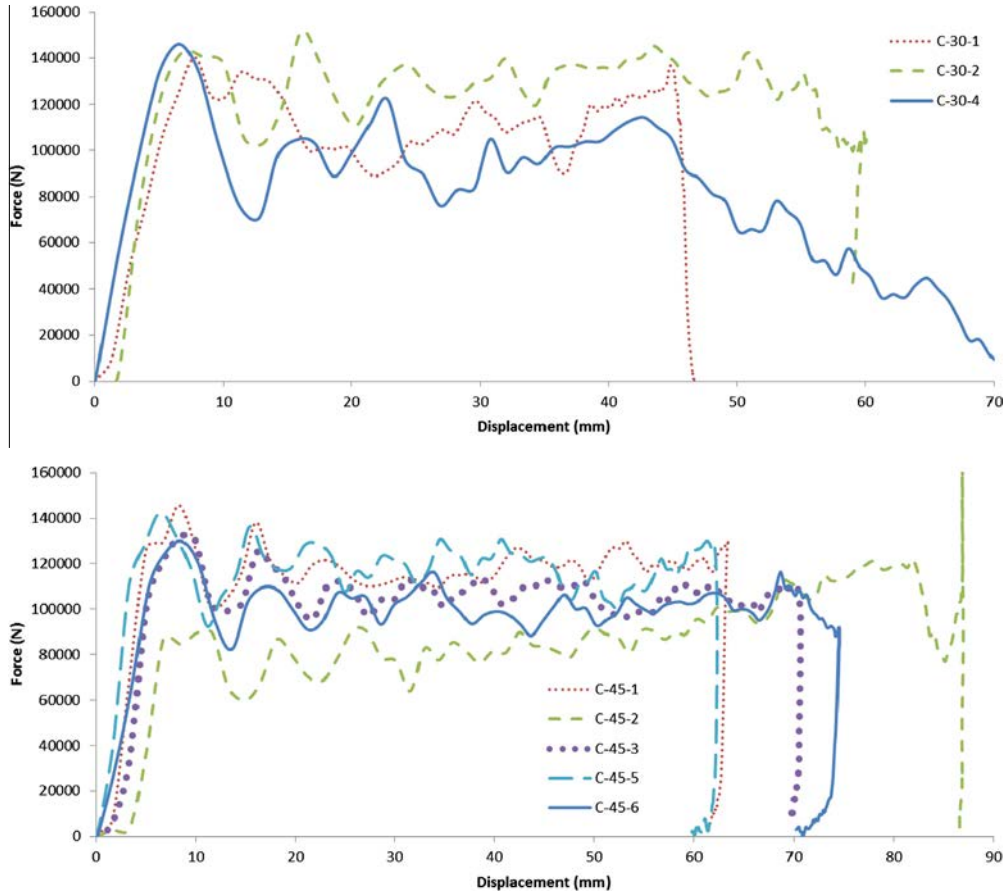


Fig. 7. Force–displacement curves for carbon/polyamide tubes (impact angle 0°) with through-the-thickness fibers orientated at $\pm 30^\circ$ (top) and $\pm 45^\circ$ (bottom).

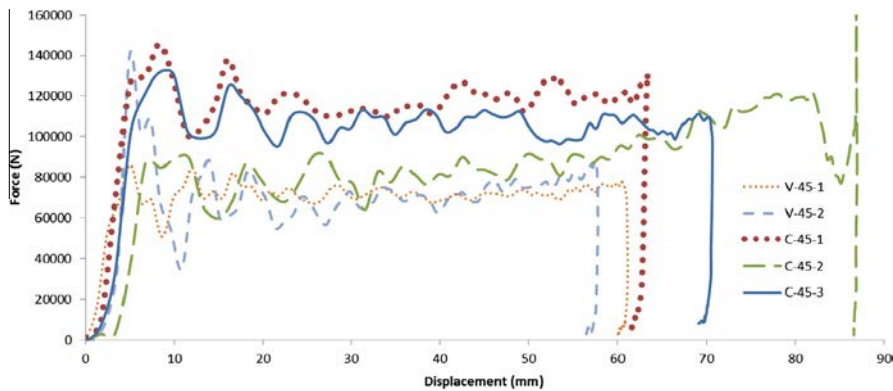


Fig. 8. Comparison of glass/polypropylene and carbon/polyamide force–displacement curves for an impact angle of 0° and fiber orientation of $\pm 45^\circ$.

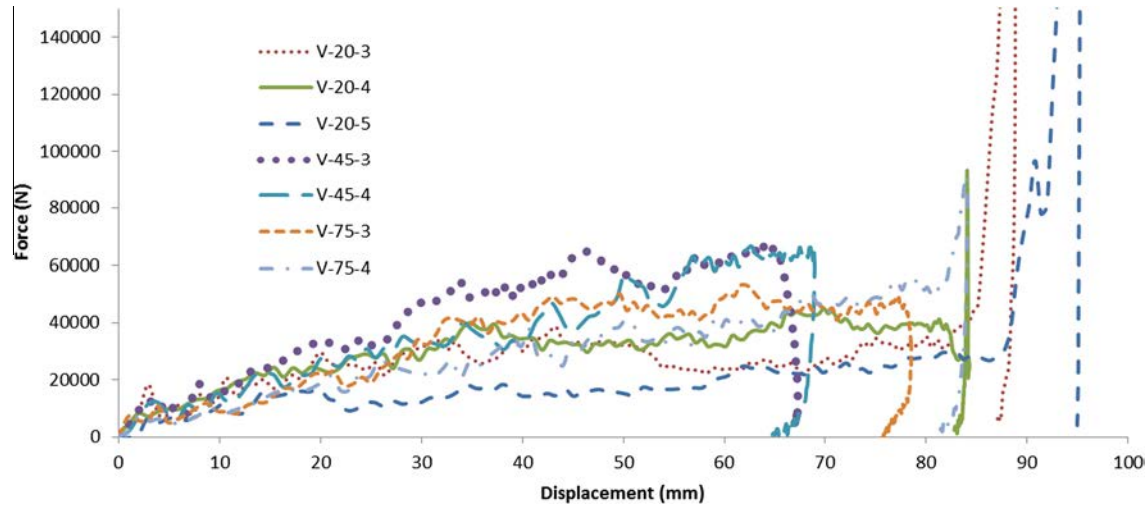


Fig. 9. Force–displacement curves for an impact angle of 15°.

Table 6

Crushing modes for carbon/polyamide tubes (impact angle 15°).

Trial	Orientation (°)	Trigger	Crushing mode
C-30-3	30	Yes	Catastrophic breaking
C-45-4	45	Yes	Catastrophic breaking

for carbon/polyamide than glass/polypropylene tubes. The amplitude of oscillations during the steady stage is also more important for carbon/polyamide tubes.

In order to confirm the influence of matrix and reinforcement materials, the force–displacement curves of carbon/polyamide and glass/polypropylene 110 mm-long $\pm 45^\circ$ fiber oriented tubes are compared in Fig. 8. This shows again that peak and average forces are higher in carbon reinforced polyamide composite tubes.

In terms of off-axis crushing, both carbon/PA and glass/PP composites tubes show a long softly increasing first part which is belatedly followed by a steady stage (Fig. 9). In some experiments, 45 mm were required before reaching the stable phase.

The steady crushing stage of all force–displacement curves shows some oscillations with certain periodicity. For progressive folding mode, a 14 mm period was recorded that may correspond to the structural pattern of the fibers. The splaying mode shows a 5 and 10 mm period, for 110 and 200 mm, respectively, long tubes. The hypothesis that this phenomenon is caused by resonance of tubes has been proved wrong by a spectral analysis using Matlab software which showed smaller periods. The 2.5D braided carbon fibers tubes show periods that range between 7 and 10 mm.

3.3. Specific energy absorption

The specific energy absorption (SEA) for all tested specimens is detailed in Tables 7 and 8. Firstly, we are interested in glass/polypropylene tubes. In terms of axial impact, the specific energy absorption increases with decreasing length-to-diameter ratio (Fig. 10 (top)) and increasing fiber orientation angle (Fig. 10 (middle)). The maximum SEA of ~ 36 kJ/kg is then achieved with short (110-mm long) tubes reinforced with fibers oriented in $\pm 75^\circ$ directions. The SEA of long tubes is 5–25% lower than that obtained with shorter specimens (Fig. 10 (top)). Tubes with $\pm 20^\circ$ fiber orientations absorb up to 30% less energy than $\pm 75^\circ$ fiber oriented tubes.

Fig. 10 (bottom) compares SEA obtained during axial and off-axis impacts. It is reported that tubes absorb 20–30% less energy during off-axis impact. The maximum SEA is obtained for $\pm 45^\circ$ fiber oriented tubes.

Table 7

Crush efficiency and specific energy absorption for glass/polypropylene composites tubes.

Trial	Orientation	Impact angle (°)	Fmax	Fave	CE	SEA
V2-20-1	20	0	81088	32153	0.40	17543
V2-20-2	20	0	85042	38324	0.45	20776
V-20-1	20	0	79160	40816	0.52	22334
V-20-2	20	0	108244	26681	0.25	14512
V-20-6	20	0	83975	49387	0.59	24311
V2-45-1	45	0	96527	49452	0.51	23097
V2-45-2	45	0	106762	46873	0.44	22408
V-45-1	45	0	87376	71351	0.82	34331
V-45-2	45	0	143432	73377	0.51	34546
V2-75-1	75	0	73753	48379	0.66	26130
V2-75-2	75	0	67213	49482	0.74	26938
V-75-1	75	0	67024	57511	0.86	34171
V-75-2	75	0	71456	64329	0.90	37676
V-20-3	20	15	40783	28237	0.69	14833
V-20-4	20	15	46752	37040	0.79	18876
V-20-5	20	15	29777	18493	0.62	8088
V-45-3	45	15	69424	58031	0.84	27048
V-45-4	45	15	68742	62910	0.92	29087
V-75-3	75	15	55620	45883	0.82	26656
V-75-4	75	15	58551	43484	0.74	24823

Table 8

Crush efficiency and specific energy absorption for carbon/polyamide composites tubes.

Trial	Orientation	Impact angle (°)	Fmax	Fave	CE	SEA
C-30-1	30	0	140254	108671	0.77	55126
C-30-2	30	0	151463	134794	0.89	70774
C-30-4	30	0	146011	98174	0.67	56470
C-45-1	45	0	145748	118716	0.81	55282
C-45-2	45	0	100737	86081	0.85	40117
C-45-3	45	0	131575	107758	0.82	50260
C-45-5	45	0	142594	119446	0.84	58431
C-45-6	45	0	129795	100311	0.77	48781

The energy absorption of carbon/polyamide tubes is depicted in Fig. 11. In opposite to glass/PP tubes, the carbon/PA SEA is decreasing with increasing orientation. The highest SEA is ~ 61 kJ/kg,

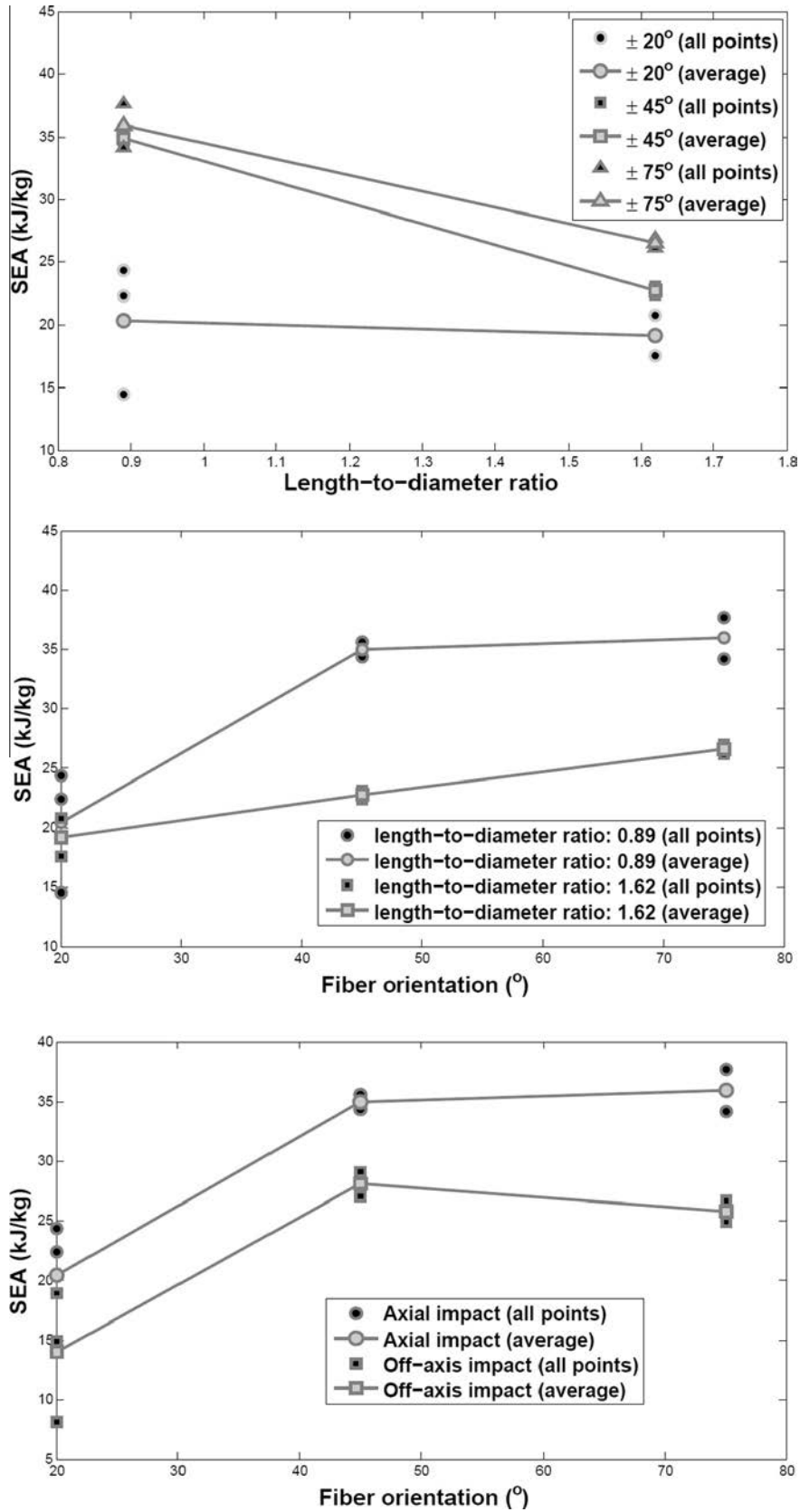


Fig. 10. Specific energy absorption for glass/polypropylene composite tubes: influence of length-to-diameter ratio (top), influence of the fiber orientation (middle) and influence of the impact angle (bottom).

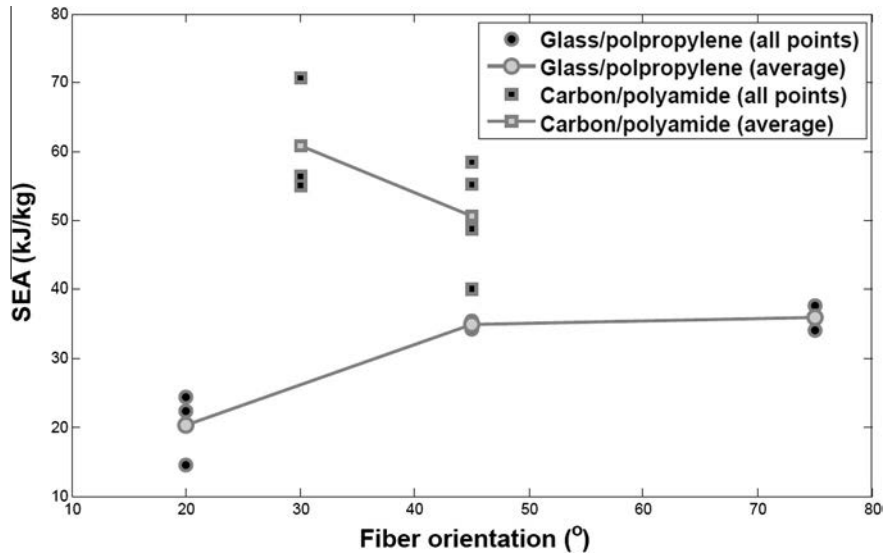


Fig. 11. Comparison of specific energy absorption of glass/polypropylene and carbon/polyamide.

which is 70% as higher as the maximum SEA obtained with glass/PP tubes. For $\pm 45^\circ$ fiber oriented tubes, carbon reinforced tubes absorb 40% more energy than glass reinforced tubes.

3.4. Crush efficiency

The crush efficiency is defined in Eq. (1) as the average-to-maximum forces ratio. In terms of crashworthiness performance, the ideal crush efficiency ratio is 1. The crush efficiency ratio (CE) of all experiments is also reported in Tables 6 and 7. This ratio is highly affected by the trigger mainly for $\pm 30^\circ$ and $\pm 45^\circ$ fiber orientation. In these architectures, triggered tubes have high CE than non-triggered ones.

The crush efficiency is also sensitive to length-to-diameter ratio and to fiber orientation. In terms of glass/PP tubes, CE increases for decreasing length-to-diameter ratio (Fig. 12 (top)) and increasing fiber orientation (Fig. 12 (middle)). The best CE (~ 0.85) is obtained for short tubes and $\pm 75^\circ$ fiber orientation. Similarly to axial impact, the crush efficiency obtained in off-axial impacts increases with increasing fiber orientation (Fig. 12 (bottom)). Fig. 13 depicts the crush efficiency of carbon/PA tubes. Contrarily to specific energy absorption, CE is increasing with increasing fiber orientation. Moreover, glass/PP and carbon/PA tubes have almost the same crush efficiency (~ 0.82) at $\pm 75^\circ$ fiber orientation.

4. Discussion

The crashworthiness efficiency of 2.5D braided thermoplastic composite tubes was investigated. The crushing modes were observed: splaying and progressive folding modes for glass/PP tubes and fragmentation for carbon/PA modes. The splaying mode is the most reported mode for braided composite tubes. It was observed for carbon/epoxy [57,61,62,64] and glass/epoxy [61,63] tubes. The folding mode is observed in Ref. [57] for braided Kevlar/epoxy tubes and in Ref. [63] for glass/epoxy tubes. The fragmentation mode was also reported in Ref. [63] for glass/epoxy tubes. Chiu et al. [55] concluded that braid yarns controls the crushing mode. This is partially confirmed in this work as braiding angle influence the crushing mode of glass/PP tubes. For low braiding angles, the transverse stiffness and strength are not significant. Therefore it is possible to tear the tube's wall to make fronds. As braiding angle increases, the transverse strength and stiffness increase. It becomes hard to tear the tube's wall. Therefore, the

progressive folding mode is privileged. This mode is close to metallic crushing mode and is rather associated to ductile behavior of fibers [57]. In the opposite, the fragmentation mode can be attributed to the brittle behavior of carbon fibers.

In this study, the fragmentation mode yields to the highest specific energy absorption. Moreover, the folding mode gives higher specific energy absorption than the splaying mode. This is opposite to observations drawn by Gui et al. [63] who have reported the splaying mode gives the highest SEA. Actually, the energy absorption capability cannot be associated to the only crushing mode. It is also influenced by matrix or fiber material, fiber architecture, trigger, etc. Moreover, the effects of these parameters should be rather coupled as for example the energy absorption is influenced by the crushing mode which also depends on fiber architecture or matrix and fiber materials.

The specific energy absorption of glass/PP and carbon/PA depends on the braiding angle. However, glass/PP SEA's is increasing whereas carbon/PA SEA's is decreasing with increasing angle. Actually, both behaviors were already reported in literature. Gui et al. [63] found that SEA for glass/epoxy tubes increases with decreasing braiding angle. Xiao et al. [64] and Flesher et al. [65] depicted that SEA increases with increasing braiding angle for carbon/epoxy tubes. Okano et al. [61] showed that SEA increases with increasing braiding angle for carbon/epoxy tubes. However, the tendency is reversed when using flexible matrix. Here also we confirm that braiding effect is coupled matrix and fiber materials. In terms of glass/polypropylene tubes, the SEA is increasing with the increase of braiding angle. This can be attributed to the increase of the transverse stiffness of the tubes. This has to be associated with the crushing mode. More precisely, the transverse stiffness opposes the tearing of tubes in the splaying mode and local buckling. The higher the transverse stiffness, the higher the specific energy will be. For the carbon/polyamide tubes, the SEA decreases with the braiding angle. This can be explained by the fact that fragmentation is caused by axial compression loads. The increase of braiding angle yields a decrease on the axial stiffness and then a decrease in the absorbed energy.

The highest SEAs for glass/PP and carbon/PA tubes are around 36 and 61 kJ/kg, respectively. This shows that thermoplastic 2.5D braided composites materials have a great potential to be use for crashworthiness applications. The SEA of glass/PP tubes is comparable to best metallic tubes SEAs as Cunat [67] showed that the SEA of steel tubes is between 12.5 and 38 kJ/kg. Bouchet et al. [68]

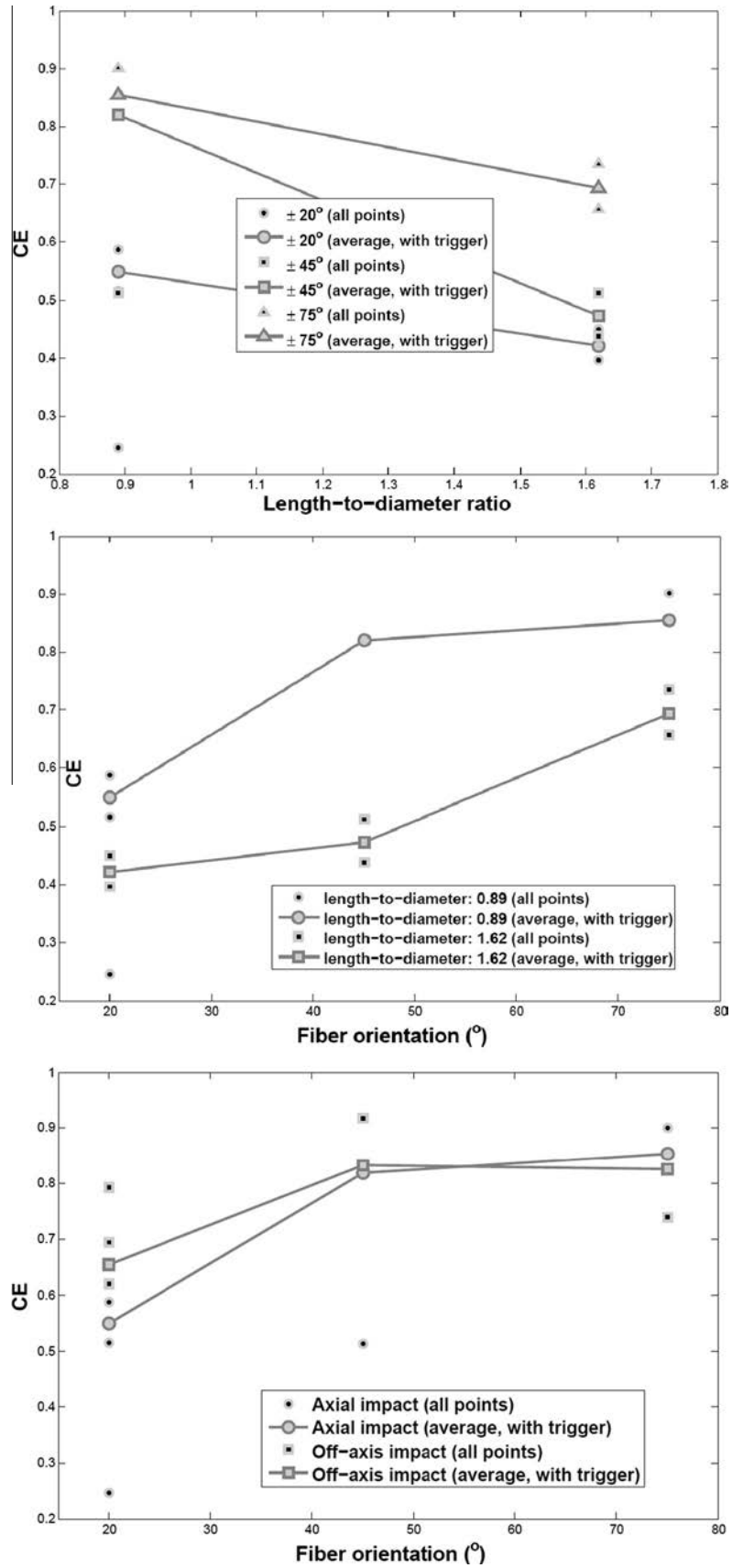


Fig. 12. Crush efficiency for glass/polypropylene composite tubes: influence of length-to-diameter ratio (top), influence of the fiber orientation (middle) and influence of the impact angle (bottom).

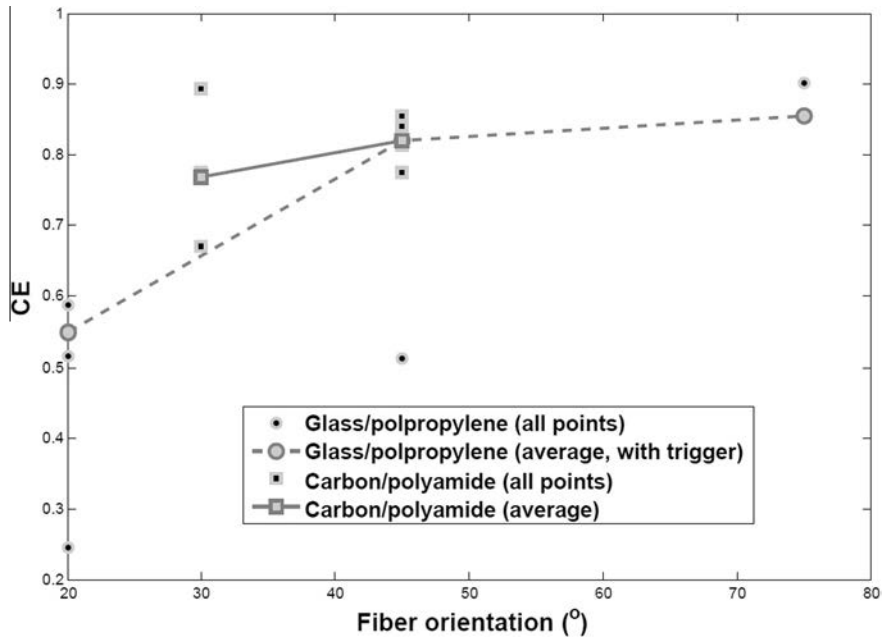


Fig. 13. Comparison of crush efficiency of glass/polypropylene (short tubes) and carbon/polyamide.

found that aluminum tube's SEA ranges from 22 to 43 kJ/kg. However, the crush force efficiency of steel and aluminum tubes was less than 0.6.

Carbon/polyamide tubes have 70% higher specific energy absorption value than glass/polypropylene. Comparable crush force efficiency was observed. Carbon/polyamide tubes used in this study had manufacturing defects that lead to catastrophic failure at off axis impacts. New results are needed to evaluate this material, but manufacturing challenges are numerous.

In terms of thermoset braided composites, the SEA of carbon/epoxy tubes ranges from 30 kJ/kg [62,64] to 87 kJ/kg [66]. On the other hand, the highest reported SEA for glass/epoxy tubes is SEA is ~ 42 kJ/kg [63].

5. Conclusions

An experimental program was carried out to investigate the crashworthiness performance 2.5D braided thermoplastic composite tubes. Two composite materials were considered. The influence of tube length and braiding angle were studied. Three crushing modes were observed: fragmentation, progressive folding and splaying modes. The fragmentation mode consists in a progressive fracturing of the composite material in small pieces. It presents the highest specific energy absorption (61 kJ/kg) and is characteristic of the carbon/polyamide braided tubes. On the other hand, the progressive folding is close to metallic tubes behavior. Several buckles appear and dissipate the crash energy. Internal damaging can occur but the structure integrity remains. It is observed for high braiding angles of glass/polypropylene composite tubes and has specific energy absorption of 36 kJ/kg. The splaying mode consists in a progressive tearing and bending of the tube's wall. Due to the through-the-thickness reinforcement, delamination is reduced, leading mainly to efficient global bending of the tube's wall and extensive internal damages. The crashworthiness performance of glass/PP tubes is comparable to best metallic and some thermoset braided composites tubes performances. The carbon/PA tubes crash energy absorption capability is comparable to performance of some thermoset braided tubes and clearly better than performance of metallic tubes. This first experimental program,

dealing with thermoplastic 2.5D braided composite tubes, showed a great potential of this type of materials in use in crash energy absorption. These results will be used for the validation of analytical and numerical models for 2.5D composites.

Acknowledgement

CETIM is highly acknowledged for the financial support of this research.

References

- [1] Barnes G, Coles I, Roberts R, Adams DO, Garner DM. Crash safety assurance strategies for future plastic and composite intensive vehicles (PCIVS). Report of U.S. department of transportation, DOT-VNTSC-NHTSA-10-01.
- [2] Yamazaki K, Han J. Maximization of the crushing energy absorption of tubes. *Struct Optim* 1998;16:37–46.
- [3] Song H, Wan Z, Xie Z, Du X. Axial impact behavior and energy absorption efficiency of composite wrapped metal tubes. *Int J Impact Eng* 2000;24:385–401.
- [4] Alghamdi AAA. Collapsible impact energy absorbers: an overview. *Thin-Walled Struct* 2001;39:189–213.
- [5] Jones N. Several phenomena in structural impact and structural crashworthiness. *Eur J Mech A/Solids* 2003;22:693–707.
- [6] El-Hage H, Mallick P, Zamani N. A numerical study on the quasi-static axial crush characteristics of square aluminum tubes with chamfering and other triggering mechanisms. *Int J Crash* 2005;10:183–96.
- [7] Nagel GM, Thambiratnam DP. Dynamic simulation and energy absorption of tapered thin-walled tubes under oblique impact loading. *Int J Impact Eng* 2006;32:1595–620.
- [8] Tarigopula V, Langseth M, Hopperstad OS, Clausen AH. Axial crushing of thin-walled high-strength steel sections. *Int J Impact Eng* 2006;32:847–82.
- [9] Olabi AG, Morris E, Hashmi MSJ. Metallic tube type energy absorbers: a synopsis. *Thin-Walled Struct* 2007;45:706–26.
- [10] Guegan P, Lebreton D, Pasco F, Othman R, Le Corre S, Poitou A. Metallic energy-absorbing inserts for Formula One tyre barriers. *Proc Inst Mech Eng, Part D: J Automob Eng* 2008;222:699–704.
- [11] Chung Kim Yuen S, Nurick GN. The energy-absorbing characteristics of tubular structures with geometric and material modifications: an overview. *Appl Mech Rev* 2008;61. 020802-20802.
- [12] Ahmed Z, Thambiratnam DP, Tan ACC. Dynamic energy absorption characteristics of foam-filled conical tubes under oblique impact loading. *Int J Impact Eng* 2010;37:475–88.
- [13] Mamalis AG, Robinson M, Manolakos DE, Demosthenous GA, Ioannidis MB, Carruthers J. Review: crashworthy capability of composite material structures. *Compos Struct* 1997;37:109–34.
- [14] Jacob JC, Simunovic JFS, Starbruck JM. Energy absorption in polymer composite for automotive crashworthiness. *J Compos Mater* 2002;36:813–50.

- [15] Thornton PH, Edwards PJ. Energy absorption in composite tubes. *J Compos Mater* 1982;16:521-45.
- [16] Farley GL. Energy absorption in composite materials. *J Compos Mater* 1983;17:267-79.
- [17] Thornton PH. The crush behavior of glass fiber reinforced plastic sections. *Compos Sci Technol* 1986;27:199-223.
- [18] Farley GL. Effect of specimen geometry on the energy absorption capability of composite materials. *J Compos Mater* 1986;20:390-400.
- [19] Thornton PH. The crush behavior of pultruded tubes at high strain rates. *J Compos Mater* 1990;24:594-615.
- [20] Hull D. A unified approach to progressive crushing of fiber-reinforced composite tubes. *Compos Sci Technol* 1991;40:377-421.
- [21] Farley GL, Jones RM. Crushing characteristics of continuous fiber-reinforced composite tubes. *J Compos Mater* 1992;26:37-50.
- [22] Mahdi E, Sultan H, Hamoua AMS, Omer AA, Mokhtar AS. Experimental optimization of composite collapsible tubular energy absorber device. *Thin-Walled Struct* 2006;44:1201-11.
- [23] Greve L, Pickett AK, Payen F. Experimental testing and phenomenological modeling of the fragmentation process of braided carbon/epoxy composite tubes under axial and oblique impact. *Compos: Part B* 2008;39:1221-32.
- [24] Feraboli P, Wade B, Deleo F, Rassian M. Crush energy absorption of composite channel section specimens. *Compos: Part A* 2009;40:1248-56.
- [25] Aljibori HSS. Energy absorption characteristics and crushing parameters of filament glass fiber/epoxy composite tubes. *Eur J Sci Res* 2010;39(1):111-21. ISSN 1450-216X 2010.
- [26] Obradovic J, Boria S, Belingardi G. Lightweight design and crash analysis of composite frontal impact energy absorbing structures. *Compos Struct* 2012;94:423-30.
- [27] Yan L, Chow N. Crashworthiness characteristics of flax fibre reinforced epoxy tubes. *Mater Des* 2013;51:629-40.
- [28] Mamalis AG, Manolakos DE, Baldoukas AK, Viegeln GL. Energy dissipation and associated failure modes when axially loading polygonal thin-walled cylinders. *Thin-Walled Struct* 1991;12:17-34.
- [29] Farley GL, Jones RM. Analogy for the effect of material and geometric variables on energy absorption capability of composite tubes. *J Compos Mater* 1992;26:78.
- [30] Mamalis AG, Manolakos DE, Ioannidis MB, Kostazos PK, Dimitriou C. Finite element simulation of the axial collapse of metallic thin-walled tubes with octagonal cross-section. *Thin-Walled Struct* 2003;41:891-900.
- [31] Mamalis AG, Manolakos DE, Ioannidis MB, Papapostolou DP. Crashworthy characteristics of axially statically compressed thin-walled square CFRP composite tubes: experimental. *Compos Struct* 2004;63:347-60.
- [32] Mamalis AG, Manolakos DE, Ioannidis MB, Papapostolou DP. The static and dynamic axial collapse of CFRP square tubes: finite element modelling. *Compos Struct* 2006;74:213-25.
- [33] Karbhari VM, Haller J. Effects of preform structure on progressive crush characteristics of flange-stiffened tubular elements. *Compos Struct* 1997;37:81-96.
- [34] Bisagni C. Experimental investigation of the collapse modes and energy absorption characteristics of composite tubes. *Int J Crash* 2009;14:365-78.
- [35] Warrior NA, Turner TA, Robitaille F, Rudd CD. Effect of resin properties and processing parameters on crash energy absorbing composite structures made by RTM. *Compos A* 2003;34:543-50.
- [36] Mamalis AG, Manolakos DE, Demosthenous GA, Ioannidis MB. Energy absorption capability of fibreglass composite square frusta subjected to static and dynamic axial collapse. *Thin-Walled Struct* 1996;25:269-95.
- [37] Mamalis AG, Manolakos DE, Ioannidis MB, Papapostolou DP. On the response of thin-walled CFRP composite tubular components subjected to static and dynamic axial compressive loading: experimental. *Compos Struct* 2005;69:407-20.
- [38] Ujihashi S, Yamanaka T, Kuroda H, Inou N. Energy-absorption abilities of CFRP cylinders during impact crushing. *Thin-Walled Struct* 1997;28:297-307.
- [39] Sigalas I, Kumosa M, Hull D. Trigger mechanisms in energy-absorbing glass cloth/epoxy tubes. *Compos Sci Technol* 1991;40:265-87.
- [40] Huang J, Wang X. On a new crush trigger for energy absorption of composite tubes. *Int J Crash* 2010;15:625-34.
- [41] Hamada H, Coppola JC, Hull D. Effect of surface treatment on crushing behaviour of glass cloth/epoxy composite tubes. *Composites* 1992;23:93-9.
- [42] Mahdi E, Sebaey TA. An experimental investigation into crushing behavior of radially stiffened GFRP composite tubes. *Thin-Walled Struct* 2014;76:8-13.
- [43] Oshkovr SA, Eshkour RA, Taher ST, Ariffin AK, Azhari CH. Crashworthiness characteristics investigation of silk/epoxy composite square tubes. *Compos Struct* 2012;94:2337-42.
- [44] Oshkovr SA, Taher ST, Oshkour AA, Ariffin AK, Azhari CH. Finite element modelling of axially crushed silk/epoxy composite square tubes. *Compos Struct* 2013;95:411-8.
- [45] Yan L, Chow N, Jayaraman K. Effect of triggering and polyurethane foam-filler on axial crushing of natural flax/epoxy composite tubes. *Mater Des* 2014;56:528-41.
- [46] Alkbir MFM, Sapuan SM, Nuraini AA, Ishak MR. Effect of geometry on crashworthiness parameters of natural kenaf fibre reinforced composite hexagonal tubes. *Mater Des* 2014;60:85-93.
- [47] Hamada H, Coppola JC, Hull D, Maekawa Z, Sato H. Comparison of energy absorption of carbon/epoxy and carbon/PEEK composite tubes. *Composites* 1992;23:245-52.
- [48] Hamada H, Ramakrishna S, Satoh H. Crushing mechanism of carbon fibre/PEEK composite tubes. *Composites* 1995;26:749-55.
- [49] Hamada H, Ramakrishna S, Maekawa Z, Sato H. Effect of cooling rate on the energy absorption capability of carbon fibre/PEEK composite tubes. *Polym Polym Compos* 1995;3:99-104.
- [50] Ramakrishna S, Hamada H, Maekawa Z, Sato H. Energy absorption behavior of carbon-fiber-reinforced thermoplastic composite tubes. *J Thermoplast Compos Mater* 1995;8:323-44.
- [51] Hamada H, Ramakrishna S. Effect of fiber material on the energy absorption behavior of thermoplastic composite tubes. *J Thermoplast Compos Mater* 1996;9:259-79.
- [52] Hamada H, Ramakrishna S, Sato H. Effect of fiber orientation on the energy absorption capability of carbon fibre/PEEK composite tubes. *J Compos Mater* 1996;30:947-63.
- [53] Zarei H, Kroger M, Albertsen H. An experimental and numerical crashworthiness investigation of thermoplastic composite crash boxes. *Compos Struct* 2008;85:245-57.
- [54] Karbhari VM, Hailer JE. Rate and architecture effects on progressive crush of braided tubes. *Compos Struct* 1998;43:93-108.
- [55] Chiu CH, Lu CK, Wu CM. Energy absorption characteristics of 3-D braided composite square tubes. *J Compos Mater* 1997;31:2309-27.
- [56] Chiu CH, Tsai KH, Huang WJ. Effects of braiding parameters on energy absorption capability of triaxially braided composite tubes. *J Compos Mater* 1998;32:1964-83.
- [57] Chiu CH, Tsai KH, Huang WJ. Crush-failure modes of 2D triaxially braided hybrid composite tubes. *Compos Sci Technol* 1999;59:1713-23.
- [58] Beard SJ, Chang FK. Energy absorption of braided composite tubes. *Int J Crash* 2002;7:191-206.
- [59] Inai R, Chirwa EC, Saito H, Uozumi T, Nakai A, Hamada H. Experimental investigation on the crushing properties of carbon fibre braided composite tubes. *Int J Crash* 2003;8:513-21.
- [60] Zeng T, Fang DN, Lu TJ. Dynamic crushing and impact energy absorption of 3D braided composite tubes. *Mater Lett* 2005;59:1491-6.
- [61] Okano M, Nakai A, Hamada H. Axial crushing performance of braided composite tubes. *Int J Crash* 2005;10:287-94.
- [62] McGregor CJ, Vaziri R, Poursartip A, Xiao X. Simulation of progressive damage development in braided composite tubes under axial compression. *Compos A* 2007;38:2247-59.
- [63] Gui LJ, Zhang P, Fan ZJ. Energy absorption properties of braided glass/epoxy tubes subjected to quasi-static axial crushing. *Int J Crash* 2009;14:17-23.
- [64] Xiao X, Botkin ME, Johnson NL. Axial crush simulation of braided carbon tubes using MAT58 in LS-DYNA. *Thin-Walled Struct* 2009;47:740-9.
- [65] Flesher NS, Chang FK, Janapala NR, Starbuck JM. A dynamic crash model for energy absorption in braided composite materials - Part II: implementation and verification. *J Compos Mater* 2011;45:867-82.
- [66] Yang Y, Wu X, Terada S, Okano M, Nakai A, Hamada H. Application of FRP in a vehicle for student formula SAE competition of Japan. *Int J Crash* 2012;17:295-307.
- [67] Cunat PJ. **Stainless steel properties for structural automotive applications. In: Metal bulletin international automotive materials conference. Cologne; 2000. p. 21-23.**
- [68] Bouchet J, Jacquelin E, Hamelin P. Static and dynamic behavior of combined composite aluminium tube for automotive applications. *Compos Sci Technol* 2000;60:1891-900.